

Soil dissimilatory nitrate reduction processes in the *Spartina alterniflora* invasion chronosequences of a coastal wetland of southeastern China: Dynamics and environmental implications

Dengzhou Gao · Xiaofei Li · Xianbiao Lin ·
Dianming Wu · Baoshi Jin · Yanping Huang ·
Min Liu · Xing Chen

Received: 19 April 2017 / Accepted: 11 October 2017 / Published online: 24 October 2017
© Springer International Publishing AG 2017

Abstract

Aims The invasion of *Spartina alterniflora* has a significant influence on soil biogeochemistry cycling in coastal wetlands. However, the roles of the *S. alterniflora* invasion chronosequence in regulating soil dissimilatory NO_3^- reduction processes (denitrification (DNF), anaerobic ammonium oxidation (ANA) and dissimilatory nitrate reduction to ammonium (DNRA)) remains unclear. The objective of this study was therefore to reveal the effects of *S. alterniflora* invasion on the soil NO_3^- reduction processes and associated gene abundance.

Methods We investigated plant biomass, soil properties, NO_3^- reduction processes and associated gene abundance of NO_3^- reduction pathways following

S. alterniflora invasion chronosequences of 6, 10, and 14 years compared to *Cyperus malaccensis* in a coastal wetland of southeastern China.

Results The *S. alterniflora* invasion generally increased plant biomass, soil water content, available substrates, *nirS*, anammox bacterial 16S rRNA and *nrfA* gene abundance, but it decreased soil bulk density. Soil DNF, ANA and DNRA rates in stands of *S. alterniflora* ranged from 1.52 to 17.58, 0.31 to 1.27 and 0.14 to 2.01 $\text{nmol N g}^{-1} \text{h}^{-1}$, respectively, which were generally higher than the values in stands of *C. malaccensis*. The soil NO_3^- reduction rates generally increased with the increasing chronosequence of invasion by *S. alterniflora*, while the changes in DNF and ANA rates were less pronounced than changes in DNRA. DNF was the dominant pathway (70.00–92.41%), and the ANA and DNRA contributed 2.49–15.27% and 5.10–20.75% to the total NO_3^- reduction, respectively. The contributions of DNF and ANA to the total NO_3^- reduction decreased slightly, while the contribution of DNRA increased remarkably after *S. alterniflora* invasion. Soil NO_3^- reduction processes were influenced by available substrates and associated microbial activities. It is estimated that an N loss of approximately $520.97 \text{ g N m}^{-2} \text{ yr}^{-1}$ in *C. malaccensis* and $794.46 \text{ g N m}^{-2} \text{ yr}^{-1}$ in *S. alterniflora* were linked to both DNF and ANA processes.

Conclusions The *S. alterniflora* invasion altered soil NO_3^- reduction processes by increasing soil microbial activities and available substrates and thus may further mediate the soil N availability in the coastal wetlands.

Responsible Editor: Paul Bodelier.

Electronic supplementary material The online version of this article (<https://doi.org/10.1007/s11104-017-3464-x>) contains supplementary material, which is available to authorized users.

D. Gao · X. Li · X. Lin · D. Wu · Y. Huang · M. Liu ·
X. Chen

School of Geographic Sciences, East China Normal University,
Shanghai 200241, China

M. Liu (✉)

Key Laboratory of Geographic Information Science (Ministry of
Education), East China Normal University, Shanghai 200241,
China

e-mail: mliu@geo.ecnu.edu.cn

B. Jin

School of Resources and Environment Science, Anqing Normal
University, Anqing 246011, China

Keywords Denitrification · Anammox · DNRA · Environmental implications · *Spartina alterniflora* · Coastal wetland

Introduction

Over the past several decades, a large amount of reactive nitrogen (N) derived from industrial and agricultural activities has been transported into coastal wetland ecosystems through rivers, groundwater runoff and atmospheric deposition (Canfield et al. 2010; Smith et al. 2015). Tidal marsh wetlands, as a prominent intermediate zone between land and sea, play an important role in N biogeochemistry cycling (Stottmeister et al. 2003; Cao et al. 2016). Therefore, microbial transformations of NO_3^- and associated environmental implications have drawn much attention toward coastal wetlands (Bernard et al. 2015; Cao et al. 2016; Zheng et al. 2016a). Soil N conversions in coastal wetland were mainly dominated by denitrification (DNF), anaerobic ammonium oxidation (ANA), and dissimilatory NO_3^- reduction to ammonium (DNRA) (Bernard et al. 2015).

Among soil dissimilatory NO_3^- reduction processes, DNF reduces NO_3^- and/or NO_2^- to N_2 and, to a lesser extent, N_2O under O_2 -limiting conditions (Seitzinger et al. 2006). In ANA, NH_4^+ is oxidized to N_2 by reducing nitrite (NO_2^-) or nitrate (NO_3^-), and this process has recently been reported in estuarine coastal environments (Trimmer and Nicholls 2009; Hou et al. 2013; Naeher et al. 2015; Zheng et al. 2016a; Cao et al. 2016). In addition, DNRA is the pathway that reduces NO_3^- into available NH_4^+ , which is retained in ecosystem (Silver et al. 2005; Huygens et al. 2007). N_2O is also produced as a side product at the NO_2^- reduction stage in the DNRA process (Kelso et al. 1997). Previous studies showed that DNF was the dominant microbial pathway of NO_3^- reduction processes in most of the aquatic ecosystems (Compton et al. 2011; Deegan et al. 2012; Deng et al. 2015; Shan et al. 2016; Zheng et al. 2016a). However, Cao et al. (2016) have found that DNRA contributed 75.7–85.9% of total NO_3^- reduction in a subtropical mangrove sediment of southeast China. Many studies have reported that DNF, ANA and DNRA are greatly affected by tidal pumping, temperature, salinity, available organic matter, total N (TN), NO_3^- and sulfide in coastal wetland ecosystems (Kraft et al. 2014; Smith et al. 2015; Zheng et al. 2016a; Cao et al. 2016). Meanwhile, DNF and DNRA compete for

NO_3^- and NO_2^- as an electron acceptor, of which DNF may be favored in NO_3^- -enriched environments, while DNRA tends to outcompete DNF in the environments with high TOC and insufficient NO_3^- (Dong et al. 2011). Additionally, it is well known that soil microbial communities play a critical role in controlling rates of NO_3^- reduction processes (Giles et al. 2012). DNF and DNRA are catalyzed by nitrate and nitrite reductase enzymes encoded by the functional bacterial genes *narG*, *napA*, *nirS*, *nirK* and *nrfA*, respectively, and their abundance indirectly indicates the activities of NO_3^- reduction processes (Yoshida et al. 2009; Hou et al. 2015; Gao et al. 2016). The rate limiting step in DNF is controlled by nitrite reductase (*Nir*) encoded by *nirS* and *nirK* genes (Ishii et al. 2014), and *nirS* is the most commonly used functional biomarker for the denitrifying bacterial community in coastal wetland ecosystems (Gao et al. 2016). For the two other processes, ANA and DNRA, copy numbers of the anammox bacterial 16S-rRNA gene and of the functional gene *nrfA*, respectively, have been found to be correlated with process rates in estuarine and coastal wetlands (Hou et al. 2015; Smith et al. 2015). Consequently, *nirS*, anammox 16S rRNA and *nrfA* genes are particularly suitable for the quantification of DNF, ANA and DNRA in coastal wetlands.

Exotic plant invasions are an urgent environmental issue and have a significant influence on native ecosystems (Didham et al. 2005; Li et al. 2009). *Spartina alterniflora*, a perennial C_4 halophyte, was intentionally introduced to the coastal region of China in 1979 for siltation promotion and coastal protection. It has covered an area of approximately 344.51 km^2 over the past 30 years, becoming the main plant along the Chinese coastal areas (Fig. S1). It now poses a threat to the sustainability of coastal wetland ecosystems (Zuo et al. 2012; Sun et al. 2015). Numerous previous studies have reported that *S. alterniflora* invasion can alter soil carbon (C) dynamics (Cheng et al. 2006; Zhang et al. 2010; Throop et al. 2013; Yang et al. 2016a), greenhouse gas emissions (Cheng et al. 2010; Chen et al. 2015; Yuan et al. 2015; Jia et al. 2016), microbial community structure (Yang et al. 2016b, c) and soil properties (Yang et al. 2016b; Yuan et al. 2014). In addition, there are a few studies on the soil N cycling affected by *S. alterniflora* invasion, and major changes were observed in the N pool, coupled nitrification-denitrification and N fixation (Hamersley and Howes 2005; Huang et al. 2016; Yang et al. 2016a). These results indicate that *S. alterniflora*

invasion can increase N accumulation and accelerate N fixation rates. However, the changes in soil NO_3^- reduction processes (DNF, ANA and DNRA) and their relative contributions to total NO_3^- reduction following *S. alterniflora* invasion chronosequences remain unclear. It was reported previously that *S. alterniflora* invasion significantly enhanced plant biomass, soil microbial diversity, total organic C (TOC) and total N pool (Yang et al. 2016a, b), which can alter DNF, ANA and DNRA processes. Thus, a better understanding of the influences of *S. alterniflora* invasion on soil DNF, ANA and DNRA processes is essential to the formation of effective strategies for the management of plant invasion in coastal wetlands.

S. alterniflora was introduced in Min River estuary in 2002, where it rapidly expanded and replaced *Cyperus malaccensis* in the middle tidal flat (Zhang et al. 2011). The Min River estuarine wetland has also received a large amount of dissolved inorganic N from upstream and tidal action, of which NO_3^- is approximately $51,125 \text{ t N yr}^{-1}$ (84.22% of the total inorganic N) (Liu et al. 2011; Fujian Provincial Oceanic and Fishery Administration 2016). Hence, we conducted an experiment to reveal the effects of *S. alterniflora* invasion on soil NO_3^- reduction processes in the Min River wetland of southeastern China. The main objectives of this study were to (1) evaluate the influences of *S. alterniflora* invasion on soil physicochemical properties, dissimilatory NO_3^- reduction processes (DNF, ANA and DNRA) and associated bacterial abundances; (2) elucidate the main environmental factors influencing the soil DNF, ANA and DNRA processes; and (3) reveal the contributions of soil DNF, ANA and DNRA to total NO_3^- reduction processes and their environmental implications in coastal wetland after *S. alterniflora* invasion.

Materials and methods

Study area, plant biomass and soil collection

The study area is located at the Min River estuarine wetland (Shanyutan wetland), Fujian Province, southeastern China ($26^\circ00'36''$ – $26^\circ03'42''\text{N}$, $119^\circ34'12''$ – $119^\circ41'40''\text{E}$, Fig. 1). This area is characterized as a typically subtropical monsoon climate with an annual temperature of 19.6°C and a precipitation 1350 mm, respectively (Zhang et al. 2015). The dominant soil type is coastal saline soil (Mou et al. 2014), and the soil

particle size distribution is 62–78% silt, 19.05–37.39% clay and 0.28–4.77% sand (Zhang et al. 2015). The region is enriched in bird and plant species, and the main vegetation types include *Phragmites australis*, *Cyperus malaccensis* and *Scirpus triqueter*, which are mainly located in high, middle and low tidal flats, respectively (Fig. 1). Exotic *S. alterniflora* was introduced to the Min River estuarine wetland in 2002, and it rapidly expanded to compete with native plants, gradually replacing *C. malaccensis* on the edge of the middle tidal flat (Fig. 1). The location of sampling with different *S. alterniflora* invasion times was identified based on a spatial overlay analysis of an aerial image in 2006, a SPOT5 image in 2010 (Zhang et al. 2011), a Landsat 8 image in 2014 and historical records. The sampling locations contained a *C. malaccensis* community (CM) and the three *S. alterniflora* communities that replaced *C. malaccensis* in 2002–2006 (SA-14), 2006–2010 (SA-10) and 2010–2014 (SA-6) (Fig. 1). Wherein CM and SA-14 consisted of 100% *C. malaccensis* and *S. alterniflora* community, respectively. While in SA-6, the marsh was split between pure *S. alterniflora* community (approximately 70%) and *C. malaccensis*-*S. alterniflora* symbiosis community (approximately 30%), and in SA-10, pure *S. alterniflora* community also predominated (>85%) over *C. malaccensis*-*S. alterniflora* symbiosis community (<15%). The pure stands of CM, SA-6, SA-10 and SA-14 community were selected as sampling sites, which has a good representativeness in different degree of *S. alterniflora* invasion. However, the Shanyutan wetland was separated by a tidal creek in the past several years, and the *C. malaccensis* in the northeast side of the tidal creek has been almost completely replaced by the *S. alterniflora* (Fig. 1), so the appropriate stands of *C. malaccensis* were located at west side of tidal creek. All sampling sites were located in the middle tidal flat with similar hydrodynamic and soil conditions. In each pure plant community stand (monoculture), three soil samples cores (0–10, 10–20, 20–30, 30–40, 40–50 cm depth) were collected randomly (the distance between replicates was approximately 60–80 m) using 10-cm-diameter stainless steel soil cylinders on July 23, 2016, and December 22, 2016, during the diurnal ebb-tide hours. The soil temperatures of every soil layer were recorded immediately. Three $0.5 \times 0.5 \text{ m}$ quadrats located 0.5 m close to the soil sample sites were also established randomly in each location to measure above-ground biomass. Corresponding root sampling blocks

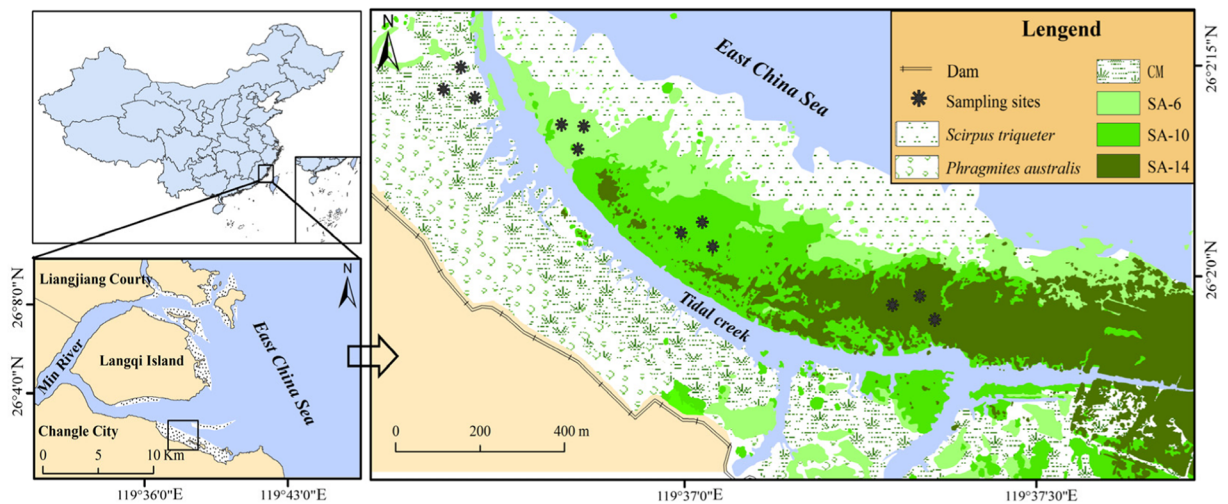


Fig. 1 Location of the study area and sampling sites. CM = *C. malaccensis*; SA-6 = *S. alterniflora* invasion 2–6 years; SA-10 = *S. alterniflora* invasion 6–10 years; SA-14 = *S. alterniflora* invasion 10–14 years

(25 cm length × 25 cm width × 25 cm depth) were excavated to measure root biomass, which represented the biomass of each stand (CM, SA-6, SA-10 and SA-14). After collection, the soil and plant samples were placed in sterile bags, sealed without air, and stored at 4 °C. All samples were transported to the laboratory for subsequent analysis within 4 h. In the laboratory, the soil samples were immediately separated into three fractions: the first fraction was freeze-dried and sieved through a 0.149-mm filter for analysis of TOC and TN; the second fraction was stored in the dark at 4 °C for measurement of soil properties and DNF, ANA and DNRA rates; and the third fraction was frozen at –80 °C for molecular analysis.

Plant biomass and soil property analysis

The plant aboveground biomass and root biomass were cleaned and oven dried at 65 °C to constant weight (Yang et al. 2016b). Soil gravimetric water content (Gravimetric water content = $(W_1 - W_2)/W_2$, W_1 = soil wet weight, W_2 = Soil dry weight) and bulk density were measured by oven drying method (60 °C, until constant weight) and a cutting-ring method, as described by Lu (2000). The soil water filled pore space (WFPS) was calculated by Nguyen et al. (2014), and the soil water was over-saturated in this study, which varied from 101.51% to 192.90% (Fig. S2). The soil pH and electrical conductivity (EC) were measured using an IQ150 instrument (IQ Scientific Instruments, USA) and a 2265FS EC meter (Spectrum Technologies Inc.,

USA), respectively (Zhang et al. 2015). Soil TN was determined using a Vario EL CN Elemental Analyzer (Elementar, Germany), and the dried soil after acidification with 1 mol L⁻¹ HCl was analyzed for TOC (Zhang et al. 2015). Soil NH₄⁺, NO₃⁻ and NO₂⁻ were extracted with 2 mol L⁻¹ KCl and measured by flow injection analysis (Skalar Analytical SAN⁺⁺, Netherlands) (Hu et al. 2016). Sulfide in soil was determined by the Methylene blue spectrophotometric method described in Lin et al. (2016).

Soil DNA extraction and quantitative PCR (q-PCR)

DNA was extracted from 0.25 g homogenized fresh soil samples using a Powersoil™ DNA Isolation Kit (MOBIO, USA) according to the manufacturer's instructions (Zheng et al. 2016a). Real-time q-PCR analysis of the extracted DNA was performed to measure the gene abundance of the NO₃⁻ reducing bacteria (*nirS* gene, anammox bacterial 16S rRNA gene and *nrfA* gene) with an ABI 7500 Detection System (Applied Biosystems, Canada) using the SYBR green method. The primers were cd3aF/R3cd for the *nirS* gene, Amx-808-F/Amx-1040-R for the anammox bacterial 16S rRNA gene, NrfAF2aw/NrfAR1 for the *nrfA* gene. The detail of the primers and q-PCR conditions for these genes are shown in Table 1. The standard curves for the *nirS* gene, anammox bacterial 16S rRNA gene and *nrfA* gene were created using a 10-fold dilution series (10²–10⁹ copies) of the standard plasmids DNA (Zheng et al. 2016a). The amplification efficiencies

Table 1 Primers and PCR conditions used in this study

| Target gene | Primers | Sequence (5'-3') | PCR conditions | Reference |
|-----------------------------|-------------------------|--|--|-------------------------|
| <i>nirS</i> gene | cd3aF R3cd | G TSAACG TSAAGGARACSGG GASTTCGGRTGSGTCTTGA | 50 °C for 2 min, 95 °C for 10 min, 45 cycles of 95 °C for 30 s, 58 °C for 40 s, 72 °C for 60 s | (Throbäck et al. 2004) |
| Anammox 16S-rRNA gene | Amx-808-F Amx-1040-R | ARCYGTAAACGATGGGCACTAA CAGCCATGCAACACCTGTRATA | 50 °C for 2 min, 95 °C for 10 min, 45 cycles of 95 °C for 30 s, 55 °C for 30 s, 72 °C for 30 s | (Hamersley et al. 2007) |
| <i>nrfA</i> gene | NrfAF2aw NrfAR1 | CARTGYCAYGTBGARTA TWNGGCATRTGRCARTC | 50 °C for 2 min, 95 °C for 10 min, 45 cycles of 95 °C for 30 s, 55 °C for 40 s, 72 °C for 30 s | (Zheng et al. 2016a) |

were 93.5%, 95.7% and 98.1% for *nirS*, anammox bacterial 16S rRNA and *nrfA* gene, respectively. These gene abundances were calculated by the constructed standard curve and then converted into copies per gram of dry soil.

Measurements of soil DNF, ANA, and DNRA rates

Soil slurry experiments were conducted to measure the potential rates of DNF and ANA by an N isotope-tracing method (Deng et al. 2015). Briefly, slurries were made by mixing fresh soil and helium-purged tidal water (30 min) at a volume ratio (soil/water) of 1:7 and then transferred into 10 respective 12-mL vials (Labco Exetainers) and sealed with a butyl rubber stopper. Subsequently, the vials were pre-incubated for 36 h to eliminate background NO_3^- , NO_2^- and O_2 in situ temperature (32 °C for summer, 17 °C for winter) in dark conditions. After the pre-incubation, these vials were spiked with sterile anoxic solutions of 100 μL of $^{15}\text{NO}_3^-$ (^{15}N at 99%) through the septa. The final concentration of ^{15}N in each vial was approximately 100 $\mu\text{mol L}^{-1}$. Then, one half of the replicates were stopped by 200 μL of 50% ZnCl_2 solution and marked as initial samples. The remaining half of the slurries were further incubated for 8 h, and these remaining sample replicates were stopped by 200 μL of 50% ZnCl_2 solution, as was described for the initial samples at the end of incubation. The concentrations of $^{29}\text{N}_2$ and $^{30}\text{N}_2$ in the vials were measured by membrane inlet mass spectrometry (MIMS), and the potential DNF and ANA rates were calculated by $^{29}\text{N}_2$ and $^{30}\text{N}_2$ production between the final and initial experimental samples (Deng et al. 2015). The occurrence of ANA at all sampling sites was confirmed by a preliminary $^{15}\text{NH}_4^+$ tracer experiment as described by Hou et al. (2013). The rates

of DNF and ANA in the slurry experiments were estimated by the accumulation of $^{29}\text{N}_2$ and $^{30}\text{N}_2$ during the slurry incubation obtained from the DNF and ANA processes, respectively, as described by Thamdrup and Dalsgaard (2002). Thus, the respective contributions of DNF and ANA to total $^{29}\text{N}_2$ production were quantified by Eq. (1)

$$P_{29} = A_{29} + D_{29} \quad (1)$$

where P_{29} ($\text{nmol N g}^{-1} \text{h}^{-1}$) denotes the total $^{29}\text{N}_2$ production rate during the slurry experiments, and D_{29} and A_{29} ($\text{nmol N g}^{-1} \text{h}^{-1}$) are the production rate of $^{29}\text{N}_2$ from DNF and the production rate of $^{29}\text{N}_2$ from ANA, respectively. ^{14}N and ^{15}N generated from $^{14}\text{NO}_3^-$ or $^{15}\text{NO}_3^-$ follow random isotope pairing (Risgaard-Petersen et al. 2003), D_{29} can be estimated by Eq. (2)

$$D_{29} = P_{30} \times 2 \times (1 - F_N) \times F_N^{-1} \quad (2)$$

where P_{30} ($\text{nmol N g}^{-1} \text{h}^{-1}$) denotes the total $^{30}\text{N}_2$ production rate and F_N (%) is the fraction of ^{15}N in NO_3^- , which can be calculated by the concentrations of added $^{15}\text{NO}_3^-$ and residual NO_3^- in the incubation slurries. Consequently, the potential rates of DNF and ANA were estimated by the Eqs. (3) and (4), respectively.

$$D_t = D_{29} + 2 \times D_{30} \quad (3)$$

$$A_{29} = P_{29} - D_{29} \quad (4)$$

where D_t and A_{29} ($\text{nmol N g}^{-1} \text{h}^{-1}$) represent the potential rates of DNF and ANA, respectively.

The DNRA of soil slurries was measured using the OX/MIMS method ($^{15}\text{NH}_4^+$ oxidation technique and MIMS analysis) reported by Yin et al. (2014). Soil slurries were prepared and preincubated, as described

for the abovementioned DNF and ANA experiments. After 36 h preincubation, 100 μL of $^{15}\text{NO}_3^-$ was injected into the slurry vials (final concentration of approximately 100 $\mu\text{mol } ^{15}\text{N L}^{-1}$ in each vial). Immediately after, one-half of the slurry was preserved with 200 μL of 50% ZnCl_2 solution as initial samples. The remaining half of the slurries were further incubated for 8 h, followed by the addition of 200 μL of 50% ZnCl_2 solution, and were designated as final samples. All slurry samples were purged by helium for approximately 30 min to eliminate the $^{29}\text{N}_2$ and $^{30}\text{N}_2$ produced by DNF and ANA during the incubation. The slurry vials were sealed, and a 100 μL hypobromite iodine solution was injected to oxidize the $^{15}\text{NH}_4^+$ (produced by DNRA) into $^{15}\text{N}_2$, and the oxide products of $^{15}\text{N}_2$ in the initial and final samples were determined by MIMS. Potential DNRA rates were estimated by $^{15}\text{NH}_4^+$ concentration changes during the incubation, which was calculated by Eq. (5)

$$R_{\text{DNRA}} = \frac{([\text{NH}_4^+]_{\text{Final}} - [\text{NH}_4^+]_{\text{Initial}}) \times V}{W \times T} \quad (5)$$

where R_{DNRA} ($\text{nmol N g}^{-1} \text{h}^{-1}$) denotes the total DNRA rate, and $[\text{NH}_4^+]_{\text{Final}}$ and $[\text{NH}_4^+]_{\text{Initial}}$ are the concentration of $^{15}\text{NH}_4^+$ in the final and initial samples of the soil slurries, respectively. $V(\text{L})$ denotes the volume of the vial, $W(\text{g})$ denotes the dry weight of the soil, and $T(\text{h})$ is the incubation time.

Statistical analysis

In the present study, the statistical analyses were performed using the SPSS 19.0 software package. The data were checked for normality and cube root- or log-converted to satisfy suppositions for statistical testing. We used repeated measures ANOVA to test the effects of season (summer and winter), degree of *S. alterniflora* invasion (CM, SA-6, SA-10 and SA-14), soil depth (0–10, 10–20, 20–30, 30–40, 40–50 cm depths) and their interactions on soil properties, gene abundance of NO_3^- reducing bacteria and NO_3^- reduction rates. Wherein soil depth was treated as within subject factor, all other factors (degree of *S. alterniflora* invasion and season) were treated as between subject factor. A within-subject-factor ANOVA and One-way ANOVA were performed to determine the significant differences in gene abundance of NO_3^- reducing bacteria and NO_3^- reduction rates at different depths in the same plant community

stands and at different plant communities stands within one depth, respectively. Pearson's correlation analysis was performed to determine the correlations among the plant biomass, soil properties, gene abundance of NO_3^- reducing bacteria and NO_3^- reduction rates.

Results

Plant biomass and soil properties

The aboveground biomass of pure *S. alterniflora* stands varied from 1272.84 to 2361.44 g m^{-2} in summer and 875.52 to 3227.24 g m^{-2} in winter, which is significantly higher than that of pure *C. malaccensis* stands (Fig. 2). The root biomass in pure *S. alterniflora* stands was also higher, although not significantly for some *S. alterniflora* sites, than that in pure *C. malaccensis* stands (Fig. 2). Significant effects of the degree of *S. alterniflora* invasion on all measured soil properties were observed (Table S1). The soil gravimetric water content, TOC, TN, $\text{NO}_3^- \text{NO}_2^-$, TOC/TN and sulfide in *S. alterniflora* were considerably higher than those of *C. malaccensis* stands, while the bulk density in *S. alterniflora* was lower than that in *C. malaccensis* (Fig. 3 and Table S2). Soil temperature, bulk density, pH, EC, TOC NO_3^- , NO_2^- and TOC/TN differed significantly by season, but there were no significant seasonal variations of water content, TN, NH_4^+ and sulfide (Table S1 and Fig. 3). Soil pH, EC, TOC, TN, NH_4^+ , NO_3^- , NO_2^- , TOC/TN or sulfide differed significantly with soil depth, and the TOC, TN, NH_4^+ , NO_3^- (apart

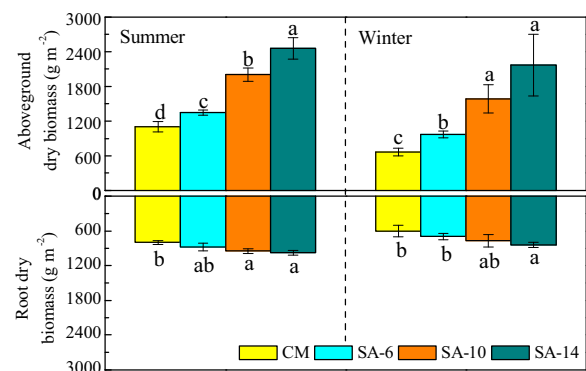


Fig. 2 Aboveground biomass and root biomass (0–25 cm soil layers) (mean \pm SE) in pure stands of *C. malaccensis* and *S. alterniflora*. Different lower case letters indicate significant differences ($p < 0.05$) at different plant community stands within the same season. See Fig. 1 for the abbreviations

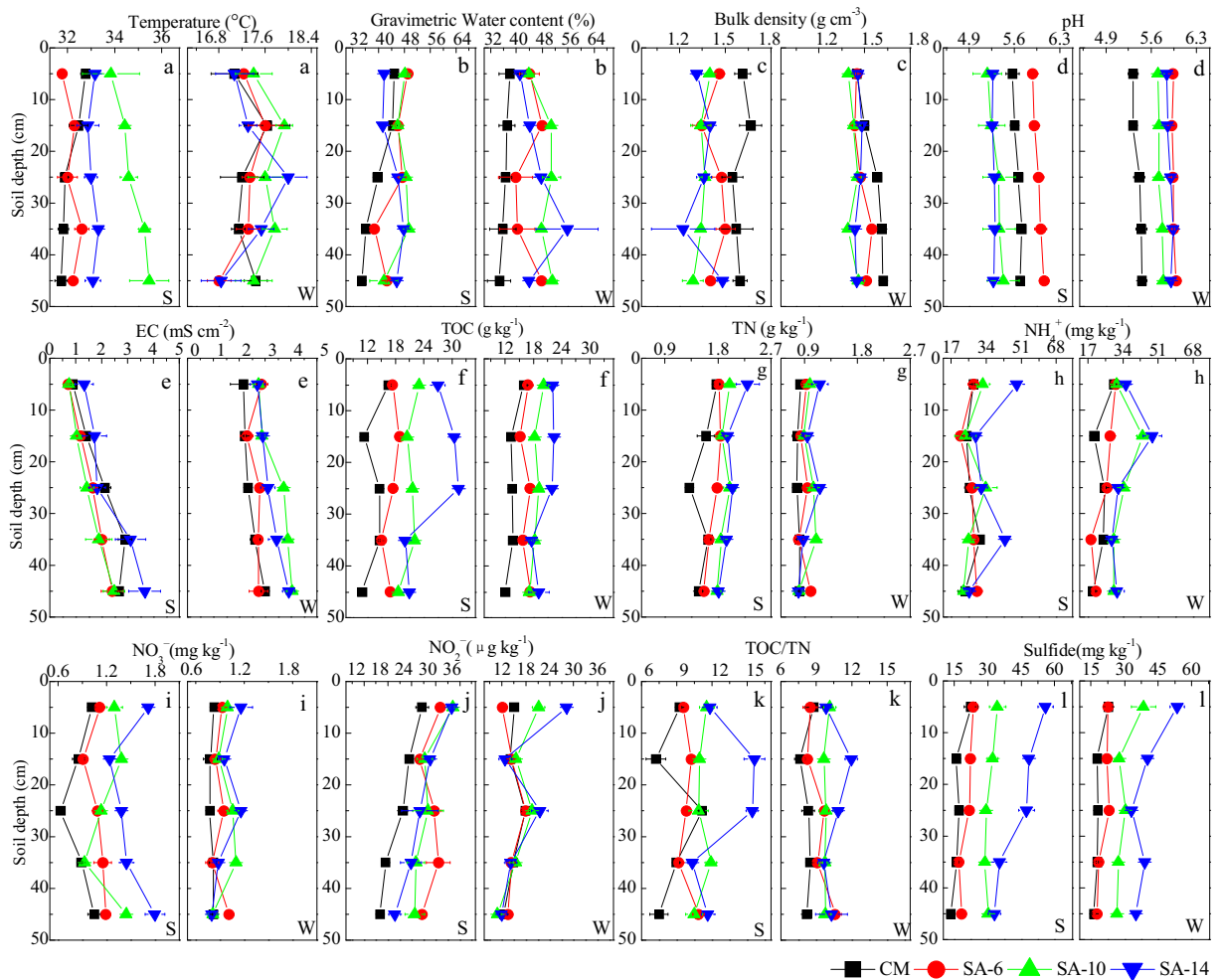


Fig. 3 The influence of *S. alterniflora* invasion, soil depth and season on soil properties (mean ± SE) (a): Temperature; b: Gravimetric water content; c: Bulk density; d: pH; e: EC; f: TOC; g: TN;

h: NH₄⁺; i: NO₃⁻; j: NO₂⁻; k: TOC/TN; l: Sulfide). S = summer, W = winter. See Fig. 1 for other abbreviations

from summer), NO₂⁻ and sulfide decreased from the upper soil layer to the deeper layer, while EC increased (Fig. 3 and Table S1).

Abundance of soil *nirS*, anammox bacterial 16S rRNA and *nrfA* gene

There were significant effects of season, degree of *S. alterniflora* invasion, soil depth and their interactions on soil *nirS*, anammox bacterial 16S rRNA and *nrfA* genes (Table S3). The gene abundances of NO₃⁻ reducing bacteria decreased with depth (except for the *nirS*-gene in summer) and were generally higher in summer than in winter (Fig. 4 and Fig. S3). The abundance of the soil *nirS* gene in *S. alterniflora* stands ranged from 6.08

to 6.34 log₁₀ copies g⁻¹ and was higher than that of *C. malaccensis* (6.0–6.19 log₁₀ copies g⁻¹) (Fig. 4i, ii). The highest abundance of the *nirS* gene was found in SA-6 in summer and in SA-14 in winter (Fig. 4i, ii). The abundance of the anammox bacterial 16S rRNA gene varied from 5.42 to 6.03 log₁₀ copies g⁻¹ in all plant community sites, and it gradually increased along the *S. alterniflora* invasion chronosequence in summer. The highest abundance of the anammox bacterial 16S rRNA gene was observed in SA-14, and there was no apparent difference among the SA-10, SA-6 and CM in winter (Fig. 4iii, iv and Fig. S3). The *nrfA* gene abundance ranged from 5.81 to 6.09 log₁₀ copies g⁻¹ in summer and 5.5 to 5.96 log₁₀ copies g⁻¹ in winter (Fig. 4v, vi). Higher *nrfA* gene abundance was recorded in

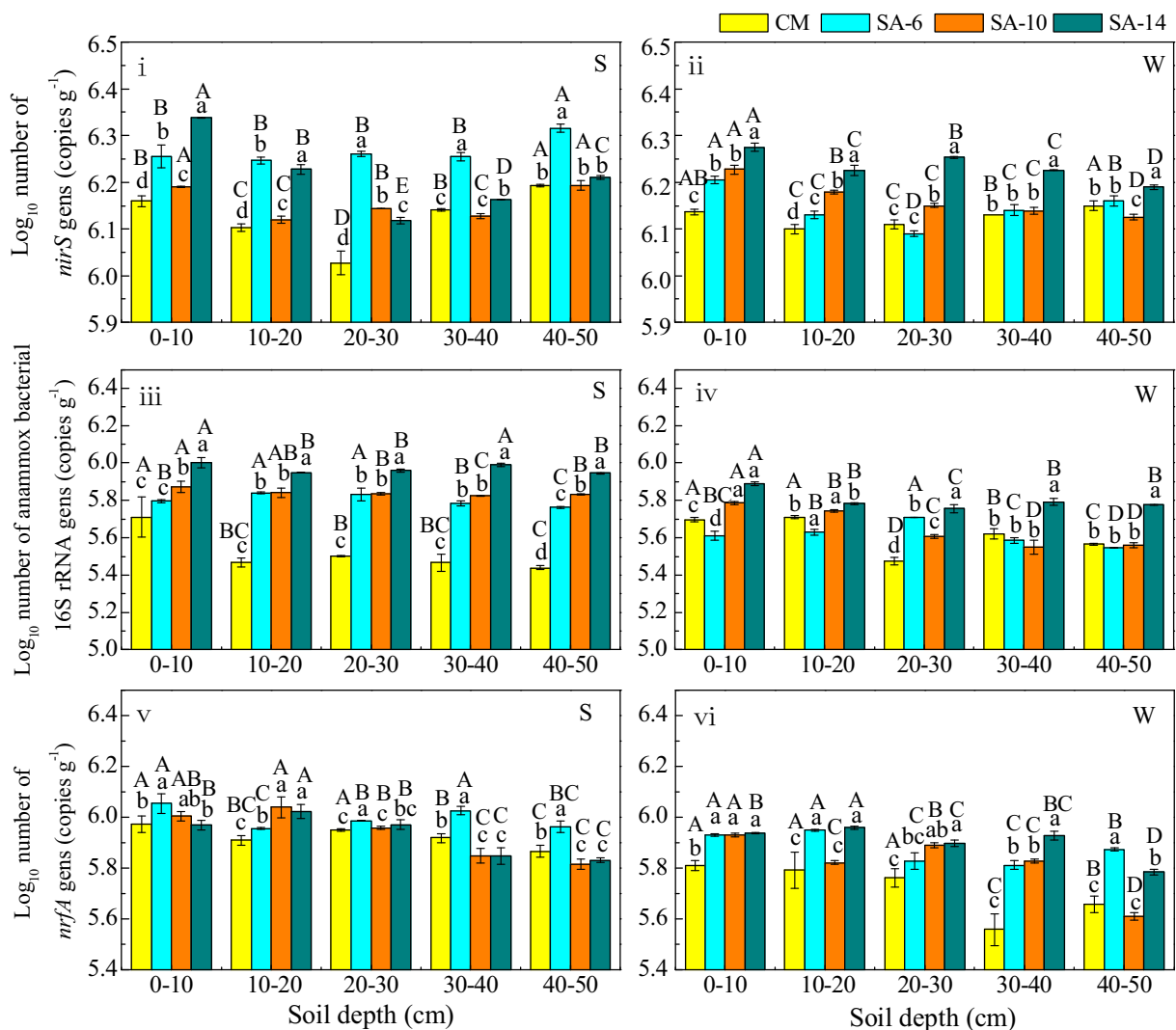


Fig. 4 The influence of *S. alterniflora* invasion, soil depth and season on soil *nirS* (i, ii), anammox bacterial 16S rRNA (iii, iv) and *nrfA* genes (v, vi) (mean \pm SE). See Figs. 1 and 3 for abbreviations. Different uppercase letters indicate significant

differences ($p < 0.05$) at different soil depths in the same plant community, and different lowercase letters indicate significant differences ($p < 0.05$) at different plant community stands within one depth

S. alterniflora compared to *C. malaccensis*, although not significantly for some *S. alterniflora* sites (Fig. 4v, vi and Fig. S3).

Potential rates of soil dissimilatory NO_3^- reduction processes

The soil dissimilatory NO_3^- reduction rates were influenced by season, degree of *S. alterniflora* invasion and soil depth (Table S4 and Fig. 5). In general, the soil DNF, ANA and DNRA rates increased with *S. alterniflora* invasion and decreased with soil depth

(Fig. 5). The soil DNF rates in *S. alterniflora* stands ranged from 8.01 to 17.57 $\text{nmol N g}^{-1} \text{h}^{-1}$ in summer and from 1.52 to 9.21 $\text{nmol N g}^{-1} \text{h}^{-1}$ in winter at the 0–40 cm soil layers. The values are generally higher than those in *C. malaccensis* (4.85 to 11.83 $\text{nmol N g}^{-1} \text{h}^{-1}$ in summer, 0.76 to 3.09 $\text{nmol N g}^{-1} \text{h}^{-1}$ in winter), and there was no significant difference in DNF rates between *C. malaccensis* and *S. alterniflora* at the 40–50 cm soil layer (Fig. 5i, ii). Notably, no significant difference was generally observed between SA-10 and SA-14 in summer and winter (Fig. 5i, ii and Fig. S4).

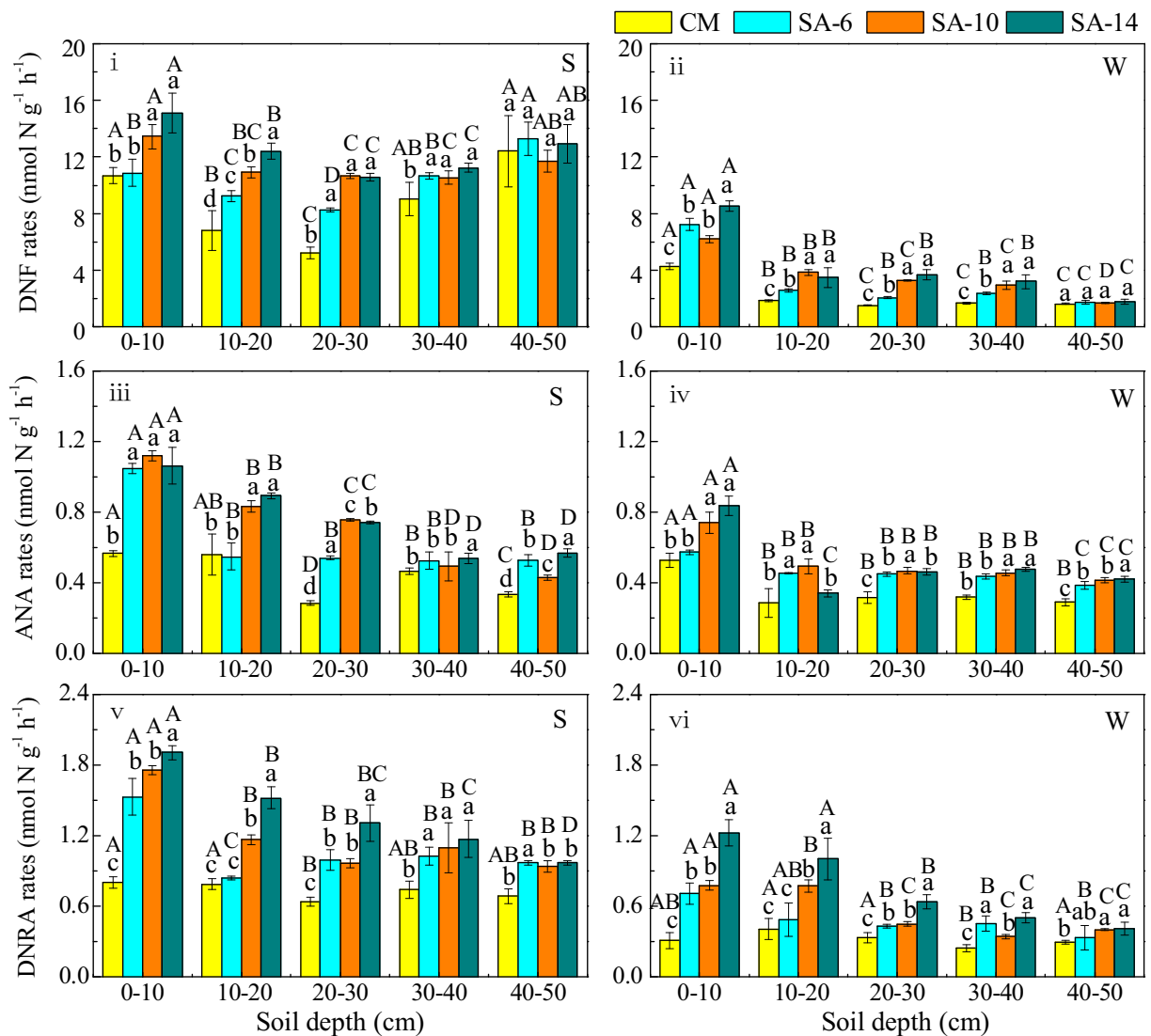


Fig. 5 The influence of *S. alterniflora* invasion, soil depth and season on soil DNF (i, ii), ANA (iii, iv) and DNRA (v, vi) (mean ± SE). See Figs. 1 and 3 for abbreviations. Different uppercase letters indicate significant differences ($p < 0.05$) at

different soil depths in the same plant community, and different lowercase letters indicate significant differences ($p < 0.05$) at different plant community stands within one depth

The soil ANA rates in *C. malaccensis* stands were 0.27–0.78 $\text{nmol N g}^{-1} \text{h}^{-1}$ in summer and 0.13–0.60 $\text{nmol N g}^{-1} \text{h}^{-1}$ in winter and showed a decreasing trend with soil depth (Fig. 5iii, iv). A similar vertical distribution pattern of soil ANA rates was also observed in *S. alterniflora* stands, ranging from 0.34 to 1.27 $\text{nmol N g}^{-1} \text{h}^{-1}$ in summer and from 0.31 to 0.92 $\text{nmol N g}^{-1} \text{h}^{-1}$ in winter (Fig. 5iii, iv). Overall, the soil ANA rates in *S. alterniflora* stands were generally higher than those of *C. malaccensis*, which was more pronounced at 0–30 cm soil depth in summer, but there was no

significant difference between SA-10 and SA-14 (Fig. 5iii, iv and Fig. S4).

Soil DNRA rates of *C. malaccensis* stands ranged from 0.56 to 0.89 $\text{nmol N g}^{-1} \text{h}^{-1}$ in summer and 0.18 to 0.53 $\text{nmol N g}^{-1} \text{h}^{-1}$ in winter. Soil depth had no significant influence on DNRA rates of *C. malaccensis* (Fig. 5v, vi). The soil DNRA rates of *S. alterniflora* stands varied from 0.42 to 2.01 $\text{nmol N g}^{-1} \text{h}^{-1}$ in summer and from 0.14 to 1.43 $\text{nmol N g}^{-1} \text{h}^{-1}$ in winter, generally exhibiting decreasing tendencies from surface to deep soil (Fig. 5v, vi). Soil DNRA rates in

S. alterniflora stands were generally higher than those in *C. malaccensis*, and this increase was more pronounced at the surface soil (0–10 cm) (Fig. 5v, vi). In addition, DNRA rates increased slightly along the *S. alterniflora* invasion chronosequence (Fig. 5v, vi and Fig. S4).

The relative contributions of DNF, ANA and DNRA to the total NO_3^- reduction processes at the 0–50 cm soil layers in study area were estimated. Soil DNF was the dominant dissimilatory NO_3^- reduction pathway, contributing 80.8–92.4% to the total NO_3^- reduction in summer and 70–85% in winter, respectively (Fig. 6). Soil ANA and DNRA were of minor importance in the NO_3^- reduction, and the contribution of ANA and DNRA to total NO_3^- reduction varied from 2.49 to 15.27% and 5.10 to 20.75%, respectively (Fig. 6). Generally, DNF contributed more NO_3^- reduction in summer than in winter, while ANA and DNRA were more important for NO_3^- reduction in winter than in summer (Fig. 6). In addition, the contribution of DNF to total NO_3^- reduction in *S. alterniflora* stands was significantly lower than that of *C. malaccensis* in summer, but it was slightly higher in *S. alterniflora* than in *C. malaccensis* in winter. The contributions of NO_3^- reduction by ANA and DNRA in *S. alterniflora* stands were generally higher than that of *C. malaccensis* in summer. In winter, the contribution of ANA to NO_3^- reduction decreased slightly along the *S. alterniflora* invasion chronosequence, but the contribution of NO_3^- reduction by DNRA varied in *C. malaccensis* and different degrees of *S. alterniflora* invasion (Fig. 6). Soil ANA was correlated with DNF and DNRA in *S. alterniflora* communities, while DNF was correlated positively with DNRA in all plant communities (Table S5). In terms of soil depth, soil DNF was correlated with ANA only in the 0–40 cm depth, while DNRA was positively correlated with DNF and ANA in all soil depths (Table S6).

Plant biomass and soil properties affecting NO_3^- reduction rates

Across the plant communities, soil DNF, ANA, DNRA, anammox bacterial 16S rRNA, bulk density, water content, TOC, TN, NH_4^+ , NO_3^- , TOC/TN and sulfide were correlated with aboveground and root biomass, while soil *nirS*, *nrfA*, temperature and NO_2^- were only correlated with root biomass (Table 2). In addition, soil DNF was positively correlated with bulk density, TOC, TN, NO_3^- , sulfide, *nirS*, and anammox bacterial 16S rRNA both in summer and winter (Table 3). Soil ANA was significantly associated with soil EC, TOC, TN, NH_4^+ , NO_3^- , NO_2^- , sulfide, anammox bacterial 16S rRNA and *nrfA* in summer, while in winter, ANA was significantly related to all measured environmental variables (except for soil temperature, pH, water content and TOC/TN) (Table 3). The DNRA rates were significantly related to TOC, TN, NH_4^+ , NO_3^- , NO_3^- , TOC/TN, sulfide, *nirS*, anammox bacterial 16S rRNA and *nrfA* in both summer and winter (Table 3).

Discussion

Effects of *S. alterniflora* invasion on soil NO_3^- reduction processes

Exotic *S. alterniflora* invasion has significant influences on plant biomass, soil nutrient availability, microbial activity and physico-chemical properties, which can feed into a series of biogeochemical processes such as soil respiration (Bu et al. 2015), N_2O emission (Jia et al. 2016), and N-fixation rates (Huang et al. 2016). Our newly revealed details show that *S. alterniflora* invasion alters soil NO_3^- reduction processes (DNF, ANA and DNRA) in estuarine wetland, which improves the

Fig. 6 The influence of *S. alterniflora* invasion and season averaged over soil depth on relative contributions of DNF, ANA and DNRA to total NO_3^- reduction (mean \pm SE). See Fig. 1 for the abbreviations. Different lowercase letters indicate significant differences ($p < 0.05$) at different plant community stands within the same season

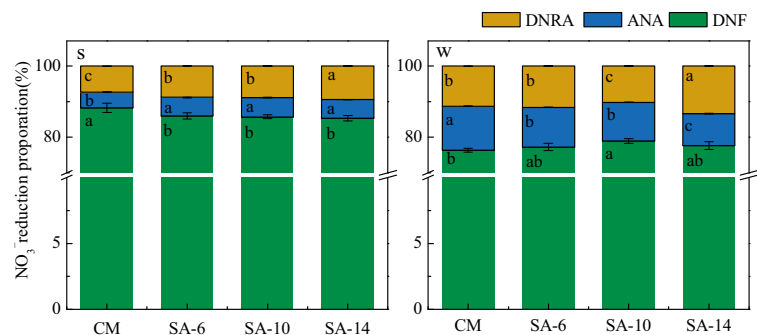


Table 2 Person's correlations of plant biomass with soil properties, gene abundance of NO_3^- reducing bacteria and NO_3^- reduction rates across the plant communities (averaged 0–50 cm soil depths)

| Soil properties | Aboveground biomass | Root biomass |
|----------------------------|---------------------|--------------|
| Temperature | n.s. | 0.592** |
| pH | n.s. | n.s. |
| EC | n.s. | n.s. |
| Bulk density | -0.612** | -0.509** |
| Water content | 0.534** | n.s. |
| TOC | 0.787** | 0.612** |
| TN | 0.629** | 0.341 |
| NH_4^+ | 0.822** | 0.499** |
| NO_3^- | 0.728** | 0.688** |
| NO_2^- | n.s. | 0.662** |
| TOC/TN | 0.779** | 0.704** |
| Sulfide | 0.823** | 0.478* |
| <i>nirS</i> | n.s. | 0.414* |
| Anammox bacterial 16S rRNA | 0.690** | 0.625** |
| <i>nrfA</i> | n.s. | 0.591** |
| DNF | 0.415* | 0.629** |
| ANA | 0.609** | 0.672** |
| DNRA | 0.604** | 0.717** |

* Significant at $p < 0.05$, ** Significant at $p < 0.01$, n.s. represent non-significant, $n = 12$

understanding of N transformations in the wetland ecosystem. In this study, we found that *S. alterniflora* invasion generally increased the soil DNF, ANA and DNRA rates compared to *C. malaccensis* (Fig. 5 and Fig. S4), which could be explained in part by the soil microbial activity and availability of soil substrates after *S. alterniflora* invasion. It has been reported that soil microbial activity is correlated with plant biomass and root systems (Welsh 2000; Zheng et al. 2016b). In the present study, plant biomass (Fig. 2) and the abundance of soil *nirS*, anammox bacterial 16S rRNA and *nrfA* genes in *S. alterniflora* sites were higher than those in the *C. malaccensis* sites (Fig. 4 and Fig. S3). A number of authors have found a positive linkage between NO_3^- reduction rates and the abundance of nitrate reducers or their functional genes (Hou et al. 2015; Smith et al. 2015; Shan et al. 2016). This was confirmed in the current study, where the process rates and the copy number of the functional genes *nirS* and *nrfA* as well as the anammox bacterial 16S rRNA genes were

significantly correlated (Table 3). However, functional *nrfA* genes were not found in all bacteria performing DNRA (Stremińska et al. 2012). Hence, the abundance and diversity of ammonifiers in estuarine wetland ecosystem needs further study. Additionally, the increase in nitrate reducer populations and the subsequent increase in process rates might also be linked to the availability of soil substrates (Smith et al. 2015; Shan et al. 2016). Many studies have reported that soil DNF and DNRA rates are affected by TOC, TN, NO_3^- , sulfide, salinity, temperature and redox environment in aquatic ecosystems (Sgouridis et al. 2011; Smith et al. 2015; Cheng et al. 2016; Shan et al. 2016). Acting as potential electron donors and substrates for both DNF and DNRA, soil TOC, sulfide and NO_3^- can ease internal competition between denitrifying and nitrate ammonifying bacteria and can promote both processes (Shan et al. 2016). This is supported by the positive correlations of the soil DNF and DNRA rates with the TOC, sulfide and NO_3^- concentrations in this study (Table 3). In addition, previous studies have indicated that the ANA process is stimulated by soil TOC, NH_4^+ , NO_3^- and NO_2^- , which may provide a favorable environment for the ANA bacterial community (Trimmer et al. 2003; Zhao et al. 2015a; Hou et al. 2015). This speculation is also supported by the positive relationships of the ANA rates with soil TOC, NH_4^+ , NO_3^- and NO_2^- (Table 3). In this study, *S. alterniflora* invasion generally increased soil TOC, TN, NH_4^+ , NO_3^- , NO_2^- and sulfide (Fig. 3, Table S2) because *S. alterniflora* has a higher litter quantity input and a higher uptake of nutrients from tidal subsidies through well-developed root systems (Huang et al. 2016; Peng et al. 2011), which further promotes DNF, ANA and DNRA rates. In addition, *S. alterniflora* invasion significantly decreased soil bulk density (Fig. 3, Table S2), which increased the O_2 concentration in the soil and therefore decreased DNF, ANA and DNRA activities. However, the importance of this mechanism may be weakened due to the compensation by increased soil respiration in *S. alternifolia* stands (Bu et al. 2015). Previous studies have reported that soil ANA might be coupled with DNF because most denitrifying bacteria are heterotrophic and capable of utilizing organic matter to generate NO_2^- and NH_4^+ , which can provide substrates for the anammox bacteria and stimulate ANA rates (Shan et al. 2016). This hypothesis is supported by the close correlation between the ANA and DNF rates in this study (Tables S5 and S6). Overall, these factors comprehensively accelerated

Table 3 Person's correlations of soil NO₃⁻ reduction rates with soil properties and gene abundance of NO₃⁻ reducing bacteria

| | Summer | | | Winter | | |
|------------------------------|-----------|-----------|------------|-----------|-----------|------------|
| | DNF rates | ANA rates | DNRA rates | DNF rates | ANA rates | DNRA rates |
| Temperature | n.s. | n.s. | n.s. | n.s. | n.s. | n.s. |
| pH | n.s. | n.s. | n.s. | n.s. | n.s. | n.s. |
| EC | n.s. | -0.612** | -0.410 | n.s. | 0.462* | n.s. |
| Water content | n.s. | n.s. | n.s. | n.s. | n.s. | n.s. |
| Bulk density | -0.444* | n.s. | n.s. | -0.523* | -0.604** | n.s. |
| TOC | 0.466* | 0.606** | 0.713** | 0.585** | 0.580** | 0.729** |
| TN | 0.525* | 0.728** | 0.736** | 0.845** | 0.822** | 0.765** |
| NH ₄ ⁺ | n.s. | 0.453* | 0.597** | 0.590** | 0.546* | 0.526* |
| NO ₃ ⁻ | 0.768** | 0.452* | 0.572** | 0.520* | 0.558* | 0.551* |
| NO ₂ ⁻ | n.s. | 0.764** | 0.763** | 0.536* | 0.671** | 0.558** |
| TOC/TN | n.s. | 0.405 | 0.534** | n.s. | n.s. | 0.469* |
| Sulfide | 0.556* | 0.642** | 0.780** | 0.679** | 0.683** | 0.809** |
| <i>nirS</i> | 0.617** | n.s. | 0.454* | 0.731** | 0.625** | 0.791** |
| Anammox bacterial 16S rRNA | 0.583** | 0.554* | 0.708** | 0.607** | 0.595** | 0.719** |
| <i>nrfA</i> | n.s. | 0.617** | 0.446* | 0.579** | 0.543* | 0.689** |

* Significant at $p < 0.05$, ** Significant at $p < 0.01$, n.s. represent non-significant, mean \pm SE for each type of stand, $n = 20$

soil dissimilatory NO₃⁻ reduction processes after *S. alterniflora* invasion.

An intriguing finding was that the extremely significant increase of in NO₃⁻ reduction by *S. alterniflora* invasion was confined to the upper 0–30 cm layer of the soil (Fig. 5). This result might be attributable to the differences in deep soil aeration between *C. malaccensis* and *S. alterniflora* stands. It has been reported that anoxic environments in coastal wetlands are conducive to NO₃⁻ reduction processes, while the loose texture and favorable aeration of soil could restrain these processes (Smith et al. 2015). In anaerobic soils, plant roots are able to transport O₂ into deeper soil layers (Popp et al. 2000), and this could potentially have a negative impact on NO₃⁻ reduction rates. *S. alterniflora* developed more roots than *C. malaccensis* (Fig. 2), leading to a potentially greater O₂ supply, which may have prevented an increase in NO₃⁻ reduction rates by *S. alterniflora* invasion in deeper soil layers. Based on the principles above, the DNF, ANA and DNRA rates in the upper soil layer should be lower because the aeration is higher there (Smith et al. 2015). However, soil NO₃⁻ reduction rates were not comparably suppressed, perhaps because of the soil substrate availability and microbial activity (Shen et al. 2015; Zheng et al. 2016a). High soil substrate availability in upper layers is favorable for

bacterial activities and soil respiration, which can consume a large amount of O₂ and counteract the effects of soil aeration (Metcalf et al. 2011). In addition, high soil substrates in upper layers can promote DNF, ANA and DNRA rates (Zheng et al. 2016a), which leads to NO₃⁻ reduction rates being generally higher in upper than deeper soil layers, generally showing a decreasing trend with soil depth. However, the decreasing of soil NO₃⁻ reduction rates from surface to deeper soil layers in *S. alterniflora* were more pronounced than in *C. malaccensis*, which might be attributable to the fact that the *S. alterniflora* invasion significantly promoted these rates in the upper soil layer. Moreover, a slight increase of DNF rates was found at 40–50 cm depth in summer (Fig. 5i), which could be explained by tidal pumping effects in coastal wetland (Zheng et al. 2016a). A large amount of NO₃⁻ is transported into estuarine wetland by Min River in summer (flood season) (Fujian Provincial Oceanic and Fishery Administration 2016), and the tide actions may cause a cyclical input of allochthonous NO₃⁻ to the deeper soil, which can stimulate nitrate and nitrite reductase enzymes and DNF rates in deeper soil in summer (Zheng et al. 2016a).

Several studies have shown that soil nutrients progressively increase along the *S. alterniflora* invasion chronosequences (Zhang et al. 2010; Yang et al.

2016b). However, in advanced stages of *S. alternifolia* invasion (SA-10 to SA-14), only DNRA but not DNF and ANA was further increased significantly (Fig. 5). Previous studies have suggested that high soil TOC and sulfide can inhibit DNF but increase DNRA, because the DNRA process uses the electron acceptor NO_3^- more efficiently in carbon-enriched environments (Risgaard-Petersen et al. 2003; Kraft et al. 2014). In addition, NO_3^- as an electron acceptor can also oxidize sulfide to sulfate in sulfide-replete environments, and sulfate as a competitive electron acceptor may inhibit DNF but promote DNRA processes (Burgin and Hamilton 2008). Moreover, suitable concentrations of TOC, NH_4^+ and NO_2^- can promote ANA rates, while high concentrations of these substrates can inhibit the ANA rates (Chamchoi et al. 2008; Bettazzi et al. 2010; Fernández et al. 2012). In this study, the highest soil TOC, NH_4^+ , NO_2^- and sulfide concentrations were observed at SA-14 (Fig. 3 and Table S2), which might have a slight inhibition effect on DNF and ANA rates but a stimulative influence on DNRA. However, further work is required to examine the effects of the availability of soil substrates on NO_3^- reduction processes.

Similar seasonal dynamics of NO_3^- reduction rates were observed in *C. malaccensis* and *S. alterniflora* wetland soils. DNF, ANA and DNRA rates were higher in summer than in winter (Fig. 5 and Fig. S4), which could be explained by the temperature changes (Canion et al. 2014). Generally, DNF, ANA and DNRA are sensitive to temperature. The optimal temperatures for DNF and ANA are approximately 25–27 °C (Canion et al. 2014) and 30–35 °C (Egli et al. 2001), respectively. Previous studies have suggested that the DNRA rate tends to increase with increasing temperature in estuarine environments (Dong et al. 2011; Smith et al. 2015). It has been documented that the soil temperatures in summer and winter in study area were 31.20–36.90 °C and 16.60–20.10 °C (Fig. 3), respectively. Hence, *S. alterniflora* invasion did not alter the seasonal changes of the soil NO_3^- reduction processes.

Environmental implications of soil NO_3^- reduction in *S. alterniflora* invasion

Reactive N production has increased from approximately 9.2 to 56 Tg y^{-1} in the past century, which has become an emerging environmental issue (Cui et al. 2013). Nearly 20% of total reactive N, mostly in the form of NO_3^- , has been transported into estuarine and coastal

wetlands. Therefore, the fate and transformation of NO_3^- have attracted much attention in this aquatic ecosystem (Cui et al. 2013). Exotic *S. alterniflora* invasion is also an urgent ecological issue in coastal wetlands (Didham et al. 2005), with a significant influence on soil DNF, ANA and DNRA processes. Meanwhile, N-enriched eutrophication in coastal wetlands promotes the invasion of *S. alterniflora* (Zhao et al. 2015b). Hence, a basic understanding of the soil NO_3^- reduction processes after *S. alterniflora* invasion and simultaneous evaluation of the contribution of each process is essential in the context of reactive N pollution and *S. alterniflora* invasion (Sun et al. 2015; Shan et al. 2016). In this study, DNF dominated the total NO_3^- reduction (80.84–92.41% for summer and 70.00–84.97 for winter), while ANA (2.49–7.79% for summer and 6.74–15.27 for winter) and DNRA (5.10–11.37% for summer and 6.09–20.75 for winter) substantially contributed to total NO_3^- reduction in *C. malaccensis* and *S. alterniflora* (Fig. 6), comparable to what has been reported in other estuarine and coastal wetlands (Smith et al. 2015; Zheng et al. 2016a). This indicates that ANA and DNRA processes should be considered when assessing the NO_3^- reduction processes in this region, especially in winter. Overall, the contribution of DNF and ANA processes to total NO_3^- reduction decreased slightly after *S. alterniflora* invasion, while the contribution of NO_3^- reduction by DNRA increased (Fig. 6), suggesting that long-term *S. alterniflora* invasion might alter the contributions of DNF, ANA and DNRA to total NO_3^- reduction processes. In this study, soil DNF rates were measured by slurry combined with ^{15}N tracer techniques based on the assumption of N_2 as an end product because the ratios of N_2O to N_2 from DNF in estuarine ecosystems are relatively low (Fig. S5) (Dong et al. 2002; Hou et al. 2014). Therefore, the slurry-based ^{15}N tracer technique is practical in the measurement of soil potential DNF rates and has already been widely applied in plains (Sgouridis et al. 2011), estuarine and coastal wetlands (Hou et al. 2015; Cao et al. 2016; Zheng et al. 2016a) and paddies (Shan et al. 2016). Soil DNRA mainly retains N in aquatic ecosystems by transforming NO_3^- into NH_4^+ , although it also a potential N-loss mechanism via N_2O production (Kelso et al. 1997). While DNRA acts as an important N-conversion mechanism, the increases in soil DNRA rates and its contribution to total NO_3^- reduction have been observed in *S. alterniflora* stands, which could indicate that *S. alternifolia* invasion likely decreases

N_2O emission (Jia et al. 2016). However, the underlying relationships between the N_2O emission and N-conversion processes remain unclear in coastal wetlands (Jia et al. 2016; Xu et al. 2017). Therefore, it is worth clarifying the effect of *S. alterniflora* invasion on N_2O emission derived from N-conversion processes in coastal wetland, as done in the following study.

Based on the average soil bulk density in stands of *C. malaccensis* (1.58 g cm^{-3}) and *S. alterniflora* (1.44 g cm^{-3}) of soil of 0–50 cm depths, it is estimated that the N losses in *C. malaccensis* and *S. alterniflora* stands were approximately $520.97 \text{ g N m}^{-2} \text{ yr}^{-1}$ (93.05% for DNF, 6.95% for ANA) and $794.46 \text{ g N m}^{-2} \text{ yr}^{-1}$ (92.93% for DNF, 7.07% for ANA), respectively (Fig. 7). These results indicate that DNF was the dominant N removal pathway, but the N removed in *S. alterniflora* marshes significantly increased by 52.50% compared to *C. malaccensis*. In addition, both of the DNF and ANA processes in *C. malaccensis* and *S. alterniflora* stands removed 1.80% and 4.00%, respectively, of the total terrigenous inorganic N from domestic, agricultural and industrial wastewater transported annually into the Min River estuary wetland, and the N loss in *S. alterniflora* stands was significantly higher than that of *C. malaccensis*. These

results indicated that if more *C. malaccensis* marshes are replaced by *S. alterniflora*, the N removal performed by microbial processes may increase significantly in the coastal wetlands. However, Huang et al. (2016) reported that *S. alterniflora* invasion may increase N fixation, which would further accelerate N pollution, and thus, the spread of *S. alterniflora* may aggravate the eutrophication in coastal ecosystems. There are still some disputes on the environmental implications of *S. alterniflora* invasion (Sun et al. 2015). Soil NO_3^- reduction is forms only a part of N-transforming biogeochemical cycles and therefore its analysis cannot comprehensively cover all aspects of *S. alterniflora* invasion. However, given the potential of both processes for N-loss (DNF and ANA) and N-conservation (DRNA) and their potential contribution to greenhouse gas emissions (N_2O), they form an important part of an ecological impact assessment.

Conclusion

The present study reported the variations of dissimilatory NO_3^- reduction processes and their environmental implications following *S. alterniflora* invasion in a

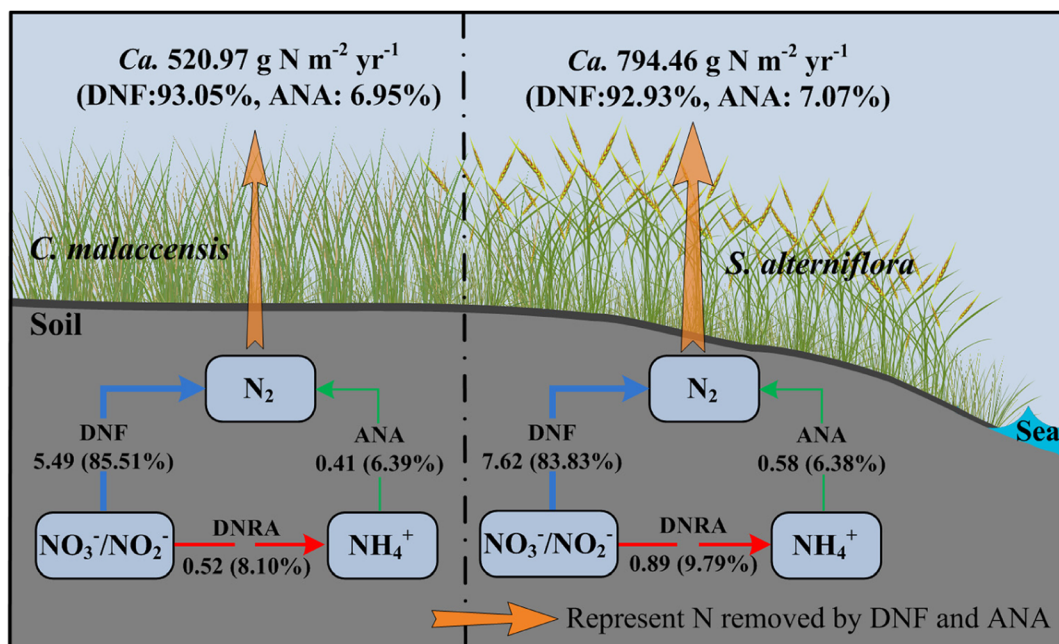


Fig. 7 A schematic illustration of soil NO_3^- reduction and total N loss in *C. malaccensis* and *S. alterniflora*. The data in the figure are the mean rates of N transformation ($\text{nmol N g}^{-1} \text{ h}^{-1}$) and their

percent contribution (%). The thickness of the arrows represents the relative importance of each rate

coastal wetland of southeastern China. Exotic *S. alterniflora* invasion significantly increased the DNF, ANA and DNRA rates compared to *C. malaccensis*. Soil NO_3^- reduction rates generally increased along the *S. alterniflora* invasion chronosequences, although DNF and ANA were less pronounced than DNRA. DNF was the dominant pathway that contributing to the total NO_3^- reduction, while ANA and DNRA played an important role in NO_3^- reduction in both the *C. malaccensis* and in *S. alterniflora* sites. The potential rates of soil DNF, ANA and DNRA rates may be affected by corresponding gene abundances of NO_3^- reducing bacteria and available substrates due to the increase in primary production and plant biomass after *S. alterniflora* invasion. It is estimated that N removal through microbial processes in *S. alterniflora* stands ($794.46 \text{ g N m}^{-2} \text{ yr}^{-1}$) is significantly higher than that of *C. malaccensis* ($520.97 \text{ g N m}^{-2} \text{ yr}^{-1}$). Overall, this study provides valuable insights into the influencing mechanism of plant invasion on soil N recycling in coastal wetlands.

Acknowledgments This work was supported by the NSFC (grant numbers: 41130525; 41371451). We thank Shixue Wu for assistance the laboratory experiments and data analyses. Many thanks are given to anonymous reviewers and editor for constructive comments and valuable suggestions on this manuscript.

References

- Bernard RJ, Mortazavi B, Kleinhuizen AA (2015) Dissimilatory nitrate reduction to ammonium (DNRA) seasonally dominates NO_3^- reduction pathways in an anthropogenically impacted sub-tropical coastal lagoon. *Biogeochemistry* 125:47–64
- Bettazzi E, Caffaz S, Vannini C, Lubello C (2010) Nitrite inhibition and intermediates effects on Anammox bacteria: a batch-scale experimental study. *Process Biochem* 45:573–580
- Bu NSQJF, Li ZL, Li G, Zhao H, Zhao B, Chen JK, Fang CM (2015) Effects of *Spartina Alterniflora* invasion on soil respiration in the Yangtze River estuary, China. *PLoS One* 10(3):e0121571
- Burgin AJ, Hamilton SK (2008) NO_3^- -driven SO_4^{2-} production in freshwater ecosystems: implications for N and S cycling. *Ecosystems* 11:908–922
- Canfield DE, Glazer AN, Falkowski PG (2010) The evolution and future of Earth's nitrogen cycle. *Science* 330:192–196
- Canion A, Overholt WA, Kostka JE, Huettel M, Lavik G, Kuypers MM (2014) Temperature response of denitrification and anaerobic ammonium oxidation rates and microbial community structure in Arctic fjord sediments. *Environ Microbiol* 16:3331–3344
- Cao WZ, Yang JX, Li Y, Liu BL, Wang FF, Chang CT (2016) Dissimilatory nitrate reduction to ammonium conserves nitrogen in anthropogenically affected subtropical mangrove sediments in Southeast China. *Mar Pollut Bull* 110:155–161
- Chamchoi N, Nitisoravut S, Schmidt JE (2008) Inactivation of ANAMMOX communities under concurrent operation of anaerobic ammonium oxidation (ANAMMOX) and denitrification. *Bioresour Technol* 99:3331–3336
- Chen YP, Chen GC, Ye Y (2015) Coastal vegetation invasion increases greenhouse gas emission from wetland soils but also increases soil carbon accumulation. *Sci Total Environ* 526:19–28
- Cheng XL, Luo YQ, Chen JQ, Lin GH, Chen JK, Li B (2006) Short-term C_4 plant *Spartina alterniflora* invasions change the soil carbon in C_3 plant-dominated tidal wetlands on a growing estuarine island. *Soil Biol Biochem* 38:3380–3386
- Cheng XL, Luo YQ, Xu Q, Lin GH, Zhang QF, Chen JK, Li B (2010) Seasonal variation in CH_4 emission and its ^{13}C -isotopic signature from *Spartina alterniflora* and *Scirpus mariqueter* soils in an estuarine wetland. *Plant Soil* 327:85–94
- Cheng L, Li XF, Lin XB, Hou LJ, Liu M, Li Y, Liu S, XTH (2016) Dissimilatory nitrate reduction processes in sediments of urban river networks: spatiotemporal variations and environmental implications. *Environ Pollut* 219:545–554
- Compton JE, Harrison JA, Dennis RL, Greaver TL, Hill BH, Jordan SJ, Walker H, Campbell HV (2011) Ecosystem services altered by human changes in the nitrogen cycle: a new perspective for US decision making. *Ecol Lett* 14:804–815
- Cui SH, Shi YL, Groffman PM, Schlesinger WH, Zhu YG (2013) Centennial-scale analysis of the creation and fate of reactive nitrogen in China (1910–2010). *Proc Natl Acad Sci U S A* 110:2052–2057
- Deegan LA, Johnson DS, Warren RS, Peterson BJ, Fleeger JW, Fagherazzi S, Wollheim WM (2012) Coastal eutrophication as a driver of salt marsh loss. *Nature* 490:388–392
- Deng FY, Hou LJ, Liu M, Zheng YL, Yin GY, Li XF, Lin XB, Chen F, Gao J, Jiang XF (2015) Dissimilatory nitrate reduction processes and associated contribution to nitrogen removal in sediments of the Yangtze estuary. *J Geophys Res Biogeosci* 120(8):1521–1531
- Didham RK, Tylianakis JM, Hutchison MA, Ewers RM, Gemmill NJ (2005) Are invasive species the drivers of ecological change. *Trends Ecol Evol* 20:470–474
- Dong LF, Nedwell DB, Underwood GJ, Thornton DC, Rusmana I (2002) Nitrous oxide formation in the Colne estuary, England: the central role of nitrite. *Appl Environ Microbiol* 68(3):1240–1249
- Dong LF, Sobey MN, Smith CJ, Sobey RI, Phillips W, Stott A, Nedwell DB (2011) Dissimilatory reduction of nitrate to ammonium, not denitrification or anammox, dominates benthic nitrate reduction in tropical estuaries. *Limnol Oceanogr* 56:279–291
- Egli K, Fanger U, Alvarez PJ, Siegrist H, van der Meer JR, Zehnder AJ (2001) Enrichment and characterization of an anammox bacterium from a rotating biological contactor treating ammonium-rich leachate. *Arch Microbiol* 175:198–207
- Fernández I, Dosta J, Fajardo C, Campos JL, Mosquera-Corral A, Méndez R (2012) Short-and long-term effects of ammonium

- and nitrite on the Anammox process. *J Environ Manag* 95: S170–S174
- Fujian Provincial Oceanic and Fishery Administration (2016) Report on the Marine Environmental Quality in Fujian in 2015. http://www.fujian.gov.cn/xw/tztl/snfw/hjqx/hyhjzl/fjshyhjzlg/201608/20160811_1208890.htm
- Gao J, Hou LJ, Zheng YL, Liu M, Yin GY, Li XF, Lin XB, Yu CD, Wang R, Jiang XF, Sun XR (2016) nirS-Encoding denitrifier community composition, distribution, and abundance along the coastal wetlands of China. *Appl Microbiol Biotechnol* 100:8573–8582
- Giles ME, Morley NJ, Baggs EM, Daniell TJ (2012) Soil nitrate reducing processes—drivers, mechanisms for spatial variation, and significance for nitrous oxide production. *Front Microbiol* 3:407
- Hammersley MR, Howes BL (2005) Coupled nitrification–denitrification measured in situ in a *Spartina alterniflora* marsh with a $^{15}\text{NH}_4^+$ tracer. *Mar Ecol Prog Ser* 299:123–135
- Hammersley MR, Lavik G, Woebken D, Rattray JE, Lam P, Hopmans EC, Sinninghe Damsté JS, Krüger S, Graco M, Gutiérrez D, Kuypers MM (2007) Anaerobic ammonium oxidation in the Peruvian oxygen minimum zone. *Limnol Oceanogr* 52(3):923–933
- Hou L, Zheng Y, Liu M, Gong J, Zhang XL, Yin GY, You L (2013) Anaerobic ammonium oxidation (anammox) bacterial diversity, abundance, and activity in marsh sediments of the Yangtze estuary. *J Geophys Res Biogeosci* 118:1237–1246
- Hou LJ, Yin GY, Liu M, Zhou JL, Zheng YL, Gao J, Zong HB, Yang Y, Gao L, Tong CF (2014) Effects of sulfamethazine on denitrification and the associated N_2O release in estuarine and coastal sediments. *Environ Sci Technol* 49(1):326–333
- Hou L, Zheng Y, Liu M, Li XF, Lin XB, Yin GY, Gao J, Deng FY, Chen F, Jiang XF (2015) Anaerobic ammonium oxidation and its contribution to nitrogen removal in China's coastal wetlands. *Sci Rep* 5:15621
- Hu M, Wilson BJ, Sun Z, Ren P, Tong C (2016) Effects of the addition of nitrogen and sulfate on CH_4 and CO_2 emissions, soil, and pore water chemistry in a high marsh of the Min River estuary in southeastern China. *Sci Total Environ* 579: 292–304
- Huang JX, Xu X, Wang M, Nie M, Qiu SY, Wang Q, Quan ZX, Xiao M, Li B (2016) Responses of soil nitrogen fixation to *Spartina alterniflora* invasion and nitrogen addition in a Chinese salt marsh. *Sci Rep* 6:20384
- Huygens D, Rütting T, Boeckx P, Van Cleemput O, Godoy R, Müller C (2007) Soil nitrogen conservation mechanisms in a pristine south Chilean Nothofagus forest ecosystem. *Soil Biol Biochem* 39(10):2448–2458
- Ishii S, Song Y, Rathnayake L, Tumendelger A, Satoh H, Toyoda S, Yoshida N, Okabe S (2014) Identification of key nitrous oxide production pathways in aerobic partial nitrifying granules. *Environ Microbiol* 16(10):3168–3180
- Jia D, Qi F, Xu X, Feng JX, Wu H, Guo JM, Peng RH, Zhu XS, Luo YQ, Lin GH (2016) Co-regulations of *Spartina Alterniflora* invasion and exogenous nitrogen loading on soil N_2O efflux in subtropical mangrove mesocosms. *PLoS One* 11(1):e0146199
- Kelso BHL, Smith RV, Laughlin RJ, Lennox SD (1997) Dissimilatory nitrate reduction in anaerobic sediments leading to river nitrite accumulation. *Appl Environ Microbiol* 63: 4679–4685
- Kraft B, Tegetmeyer HE, Sharma R, Klotz MG, Ferdelman TG (2014) The environmental controls that govern the end product of bacterial nitrate respiration. *Science* 6197:676–679
- Li B, Liao CH, Zhang XD, Chen HL, Wang Q, Chen ZY, Gan XJ, JH W, Zhao B, Ma ZJ, Cheng XL, Jiang LF, Chen JK (2009) *Spartina alterniflora* invasions in the Yangtze River estuary, China: an overview of current status and ecosystem effects. *Ecol Eng* 35:511–520
- Lin XB, Hou LJ, Liu M, Li XF, Zheng YL, Yin GY, Gao J, Jiang XF (2016) Nitrogen mineralization and immobilization in sediments of the East China Sea: spatiotemporal variations and environmental implications. *J Geophys Res Biogeosci* 121:2842–2855
- Liu XJ, Duan L, Mo JM, EZ D, Shen JL, XK L, Zhang Y, Zhou XB, He CE, Zhang FS (2011) Nitrogen deposition and its ecological impact in China: an overview. *Environ Pollut* 159: 2251–2264
- Lu LK (2000) Analysis methods of soil and agro-chemistry. China Agriculture Press, Beijing
- Metcalfe DB, Fisher RA, Wardle DA (2011) Plant communities as drivers of soil respiration: pathways, mechanisms, and significance for global change. *Biogeosciences* 8(8):2047–2061
- Mou X, Liu XT, Tong C, Sun ZG (2014) Responses of CH_4 emissions to nitrogen addition and *Spartina Alterniflora* invasion in Minjiang River estuary, southeast of China. *Chin Geogr Sci* 24(5):562–574
- Naeyer S, Huguet A, Roose-Amsaleg CL, Laverman AM, Fosse C, Lehmann MF, Derenne S, Zopfi J (2015) Molecular and geochemical constraints on anaerobic ammonium oxidation (anammox) in a riparian zone of the seine estuary (France). *Biogeochemistry* 123(1–2):237–250
- Nguyen DH, Biala J, Grace PR, Scheer C, Rowlings DW (2014) Greenhouse gas emissions from sub-tropical agricultural soils after addition of organic by-products. *SpringerPlus* 3(1):491
- Peng RH, Fang CM, Li B, Chen JK (2011) *Spartina alterniflora* invasion increases soil inorganic nitrogen pools through interactions with tidal subsidies in the Yangtze estuary, China. *Oecologia* 165:797–807
- Popp TJ, Chanton JP, Whiting GJ, Grant N (2000) Evaluation of methane oxidation in the rhizosphere of a *Carex* dominated fen in northcentral Alberta, Canada. *Biogeochemistry* 51: 259–281
- Risgaard-Petersen N, Nielsen LP, Rysgaard S, Dalsgaard T, Meyer R, L (2003) Application of the isotope pairing technique in sediments where anammox and denitrification coexist. *Limnol. Oceanogr-Me* 1: 63–73
- Seitzinger S, Harrison JA, Böhlke JK, Bouwman AF, Lowrance R, Peterson B, Tobias C, Van Drecht G (2006) Denitrification across landscapes and waterscapes: a synthesis. *Ecol Appl* 16:2064–2090
- Sgouridis F, Heppell CM, Wharton G, Trimmer M (2011) Denitrification and dissimilatory nitrate reduction to ammonium (DNRA) in a temperate re-connected floodplain. *Water Res* 45:4909–4922
- Shan J, Zhao X, Sheng R, Xia YQ, Ti CP, Quan XF, Wang SW, Wei WX, Yan XY (2016) Dissimilatory nitrate reduction processes in typical Chinese Paddy soils: rates, relative contributions, and influencing factors. *Environ Sci Technol* 50: 9972–9980

- Shen LD, Liu S, He ZF, Lian X, Huang Q, He YF, Lou LP, XY X, Zheng P, BL H (2015) Depth-specific distribution and importance of nitrite-dependent anaerobic ammonium and methane-oxidising bacteria in an urban wetland. *Soil Biol Biochem* 83:43–51
- Silver WL, Thompson AW, Reich A, Ewel JJ, Firestone MK (2005) Nitrogen cycling in tropical plantation forests: potential controls on nitrogen retention. *Ecol Appl* 15(5):1604–1614
- Smith CJ, Dong LF, Wilson J, Stott A, Osborn AM, Nedwell D (2015) Seasonal variation in denitrification and dissimilatory nitrate reduction to ammonia process rates and corresponding key functional genes along an estuarine nitrate gradient. *Front Microbiol* 6:542
- Stottmeister U, Wießner A, Kusch P, Kappelmeyer U, Kästner M, Bederski O, Müller RA, Moormann H (2003) Effects of plants and microorganisms in constructed wetlands for wastewater treatment. *Biotechnol Adv* 22:93–117
- Stremińska MA, Felgate H, Rowley G, Richardson DJ, Baggs EM (2012) Nitrous oxide production in soil isolates of nitrate-ammonifying bacteria. *Environ Microbiol Rep* 4(1):66–71
- Sun ZG, Sun WG, Tong C, Zeng CS, Yu X, Mou XJ (2015) China's coastal wetlands: conservation history, implementation efforts, existing issues and strategies for future improvement. *Environ Int* 79:25–41
- Thamdrup B, Dalsgaard T (2002) Production of N₂ through anaerobic ammonium oxidation coupled to nitrate reduction in marine sediments. *Appl Environ Microbiol* 68:1312–1318
- Throbäck IN, Enwall K, Jarvis Å, Hallin S (2004) Reassessing PCR primers targeting *nirS*, *nirK* and *nosZ* genes for community surveys of denitrifying bacteria with DGGE. *FEMS Microbiol Eco* 49(3):401–417
- Throop HL, Lajtha K, Kramer M (2013) Density fractionation and ¹³C reveal changes in soil carbon following woody encroachment in a desert ecosystem. *Biogeochemistry* 112:409–422
- Trimmer M, Nicholls JC (2009) Production of nitrogen gas via anammox and denitrification in intact sediment cores along a continental shelf to slope transect in the North Atlantic. *Limnol.Oceanogr* 54(2):577–589
- Trimmer M, Nicholls JC, Deflandre B (2003) Anaerobic ammonium oxidation measured in sediments along the Thames estuary. *United Kingdom Appl Environ Microb* 69:6447–6454
- Welsh DT (2000) Nitrogen fixation in seagrass meadows: regulation, plant–bacteria interactions and significance to primary productivity. *Ecol Lett* 3:58–71
- Xu XWH, GH F, Zou XQ, Ge CD, Zhao YF (2017) Diurnal variations of carbon dioxide, methane, and nitrous oxide fluxes from invasive *Spartina Alterniflora* dominated coastal wetland in northern Jiangsu Province. *Acta Oceanol Sin* 36(4):105–113
- Yang W, An SQ, Zhao H, LQ X, Qiao WJ, Chen XL (2016a) Impacts of *Spartina alterniflora* invasion on soil organic carbon and nitrogen pools sizes, stability, and turnover in a coastal salt marsh of eastern China. *Ecol Eng* 86:174–182
- Yang W, Jeelani N, Leng X, Chen XL, An SQ (2016b) *Spartina alterniflora* invasion alters soil microbial community composition and microbial respiration following invasion chronosequence in a coastal wetland of China. *Sci Rep* 6: 26880
- Yang W, Yan YE, Jiang F, Leng X, Chen XL, An SQ (2016c) Response of the soil microbial community composition and biomass to a short-term *Spartina alterniflora* invasion in a coastal wetland of eastern China. *Plant Soil* 408:443–456
- Yin GY, Hou LJ, Liu M, Liu ZF, Gardner WS (2014) A novel membrane inlet mass spectrometer method to measure ¹⁵NH₄⁺ for isotope-enrichment experiments in aquatic ecosystems. *Environ Sc technol* 48:9555–9562
- Yoshida M, Ishii S, Otsuka S, Senoo K (2009) Temporal shifts in diversity and quantity of *nirS* and *nirK* in a rice paddy field soil. *Soil Biol Biochem* 41:2044–2051
- Yuan JJ, Ding WX, Liu DY, Xiang J, Lin YX (2014) Methane production potential and methanogenic archaea community dynamics along the *Spartina alterniflora* invasion chronosequence in a coastal salt marsh. *Appl Microbiol Biotechnol* 98:1817–1829
- Yuan JJ, Ding WX, Liu DY, Kang H, Freeman C, Xiang J, Lin YX (2015) Exotic *Spartina Alterniflora* invasion alters ecosystem–atmosphere exchange of CH₄ and N₂O and carbon sequestration in a coastal salt marsh in China. *Glob Chang Biol* 21:1567–1580
- Zhang YH, Ding WS, Luo JF, Donnison A (2010) Changes in soil organic carbon dynamics in an eastern Chinese coastal wetland following invasion by a C₄ plant *Spartina alterniflora*. *Soil Biol Biochem* 42:1712–1720
- Zhang WL, Zeng C, Tong C, Zhang ZC, Huang JF (2011) Analysis of the expanding process of the *Spartina Alterniflora* salt marsh in Shanyutan wetland, Minjiang River estuary by remote sensing. *Procedia Environ Sci* 10: 2472–2477
- Zhang WL, Zeng CS, Tong C, Zhai SJ, Lin X, Gao DZ (2015) Spatial distribution of phosphorus speciation in marsh sediments along a hydrologic gradient in a subtropical estuarine wetland, China. *Estuar Coast Shelf Sci* 154:30–38
- Zhao H, Yang W, Xia L, Qiao YJ, Xiao Y, Cheng XL (2015a) An SQ (2015b) nitrogen-enriched eutrophication promotes the invasion of *Spartina alterniflora* in coastal China. *Clean Soil Air Water* 43(2):244–250
- Zhao JW, Zhu DW, Fan JN, Huang YM, Zhou WB (2015b) Seasonal variation of ANAMMOX and denitrification in sediments of two eutrophic urban lakes. *Pol J Environ Stud* 24:2779–2783
- Zheng YL, Hou LJ, Liu M, Liu ZF, Li XF, Lin XB, Yin GY, Gao J, CD Y, Wang R, Jiang XF (2016a) Tidal pumping facilitates dissimilatory nitrate reduction in intertidal marshes. *Sci Rep* 6:21338
- Zheng YL, Hou LJ, Liu M, Yin GY, Gao J, Jiang XF, Lin XB, Li XF, Yu CD, Wang R (2016b) Community composition and activity of anaerobic ammonium oxidation bacteria in the rhizosphere of salt-marsh grass *Spartina Alterniflora*. *Appl Microbiol Biot* 100(18):8203–8212
- Zuo P, Zhao SH, Liu CA, Wang CH, Liang YB (2012) Distribution of *Spartina* spp. along China's coast. *Ecol Eng* 40:160–166